CALCULATION OF THE GAS DYNAMICS OF COMPRESSION IN A CYLINDER OF AN INTERNAL COMBUSTION ENGINE WITH COMBUSTION CHAMBERS OF DIFFERENT SHAPE

M. A. Gorokhovskii and V. P. Khlynin UDC 517.944:532.525.6

The velocity and temperature fields for different shapes of the surface of the cylinder are presented. The computed and experimental average profiles of the velocity and intensity of turbulence are compared.

The increasingly more stringent requirements on the powers and technical and economic indicators of internal combustion engines (ICEs) stimulate the search for reserve capacity and new solutions in the organization of the working process in the construction of such engines. This requires a mathematical analysis of the processes occurring in ICEs. Computational modeling reduces the expensive and protracted work that must be performed in order to produce the engines and to modify existing engines.

Important aspects of the gas dynamics in ICEs and of combustion are studied in detail in several reviews. They concern the early work on multidimensional modeling [1-4], the question of determining turbulence in ICEs [5, 6], as well as numerical methods for calculating flows in ICEs [7, 8]. The classification of mathematical models of processes occurring in the cylinders of an engine is discussed, for example, in [9].

An important period in the operating cycle of an ICE is the compression stroke, during which the flow "controlling" the mixing and stabilization of the burning of the fuel is formed. The configuration of the flow during compression is determined, for example, by structural elements, such as the geometric shape of the combustion chamber (CC). The search for the optimal construction of the CC must contend with the need for increasing the intensity of turbulence and therefore increasing the rate of mixing of the evaporating fuel with air.

We shall study a symmetric flow of viscous compressible gas which is initiated by the translational motion of a piston whose surface, like the surface of the cylinder head, can in the general case be arbitrary. At the initial moment t = 0 the gas has zero translational velocity at a temperature of T_0 = 300 K. It is assumed that the charge rotates as a "rigid body" in a plane normal to the axis of the cylinder, i.e., the velocity, pressure, temperature, etc., remain constant along circles centered on the axis of symmetry. The effective coefficient of turbulent mixing is calculated either following the "simplified subgrid" model of turbulence [10, 11]

$$\mu_{\text{т}} = \frac{k^2}{\sqrt{2}}\rho l^2 (\tilde{D}:\tilde{D})^{1/2} \text{ with } k = 0{,}17, \tag{1}$$

or on the basis of the "differential subgrid" model of turbulence [12] with the same transport equation for the kinetic energy of subgrid turbulent scales q:

$$\mu_{\text{т}} = A\rho l q^{1/2} \quad \text{with} \quad A = 0{,}05, \tag{2}$$

$$\frac{\partial}{\partial t}(\rho q) + \nabla\cdot(\rho q \mathbf{u}) = -\frac{2}{3}\rho q \nabla\cdot\mathbf{u} + \tilde{\sigma}:\nabla\mathbf{u} + \nabla\cdot(\mu_{\text{т}}\nabla q) - \hat{D}\rho l^{-1} q^{3/2} \text{ with } \hat{D} = 1. \tag{3}$$

The symbols in Eqs. (1)-(3) were taken from [12] (the tilde denotes tensor quantities): $\tilde{D} = \nabla\mathbf{u} + (\nabla\mathbf{u})^T$; σ is the tensor of turbulent stresses and is related with the turbulent viscosity by the generalized Newton's law; ℓ is the longest side of the cell; and u is the

---

S. M. Kirov Kazakh State University, Alama-Ata. Translated from Inzhenerno-Fizicheskii Zhurnal, Vol. 57, No. 2, pp. 285-291, August, 1989. Original article submitted July 15, 1988.

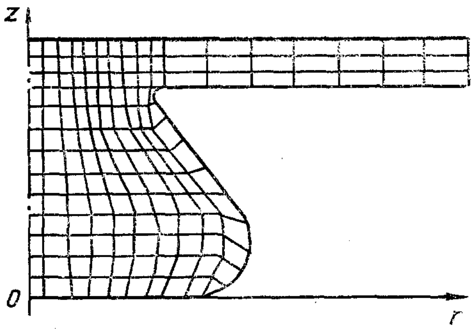

Fig. 1. Example of the configuration of the computational grid.

velocity vector averaged over the scale of the finite-difference grid. The terms on the right side of Eq. (3) denote the forces of compression, shear generation, diffusion transport, and dissipative decay of turbulence, respectively.

The velocity of the piston obeys a sinusoidal dependence: $V_p = S\pi N \sin(\alpha)(2/S + \cos(\alpha)/d)/60$. The equations employed and the mathematical formulation of the problem are given, for example, in [9].

The limited size of the working memory of the BESM-6 computer does not permit using the number of computational nodes necessary for a very thin [13] boundary layer in a cylinder of the ICE. The boundary layer on the walls of the cylinder is much thinner than the layer near the walls of the computational cells, and psoing the conditions of sticking on the wall that are standard in classical hydromechanics leads to a loss of information about the flow near the wall.

In [14, 15] the "Couette" approach to posing the boundary conditions at the wall was developed as an alternative approach to the solution of this problem. It consists of using functions "at the walls," obtained under the assumption of a laminar or turbulent Couette flow in the layer of the cells near the wall. Of course, this approach is valid for flows that do not have recirculation zones. When return flows arise there are sections on the surface of the cylinder where such an approach is obviously incorrect. However, one can hope that the errors made in posing such boundary conditions do not affect the overall geometry of the flow.

The numerical integration algorithm developed in [16-18] employs the explicit—implicit method ICE [19, 20] for tetragonal cells of arbitrary shape, which determine the spatial differences. The combined method of separation according to physical processes ICE-ALE [21, 22] involves three stages that are coupled at each time layer. At the first stage a Lagrangian calculation of the hydro- and thermodynamic parameters of the flow is performed. At the second stage an iteration procedure is employed to refine the pressure and internal-energy fields. At the third stage the individual variables are recalculated owing to convective transport.

Methods for controlling the distribution of the internal nodes of a computational grid which covers a region of arbitrary shape are well known in the literature [23-25]. For the range of problems studied the geometry of the boundaries is such that it is possible to employ simplified algorithms for the distribution of the internal nodes of the grid [23]. An example of a finite-difference grid with curvilinear boundaries, suitable for calculating ICE with a CC with a definite shape, is shown in Fig. 1.

Figure 2 shows the results of the comparison of a numerical analysis of the gas-dynamics of compression with the experimental distributions taken from [26]. The computed and experimental average values of the u component of the velocity vector are compared at the top of the figure and the average values of the v component are compared at the bottom of the figure. As one can see from Fig. 2a, modeling the boundary conditions with the help of functions "at the wall" makes it possible to reproduce the real configuration of the flow — the experimental profiles agree with the computed profiles; this confirms the existence of a thin boundary layer at the wall of the cylinder. Imposing sticking conditions at the wall, however, distorts the real pattern of the flow. As one can see, as the "resolution" of the grid is increased the solution with the sticking condition at the wall approaches the experimental profile. The experimental and computed distributions of the u and v components of the velocity, corresponding to a different mathematical formulation of the description of turbulent diffusion, are compared in Fig. 2b. To calculate the turbulent viscosity either a "simpli-

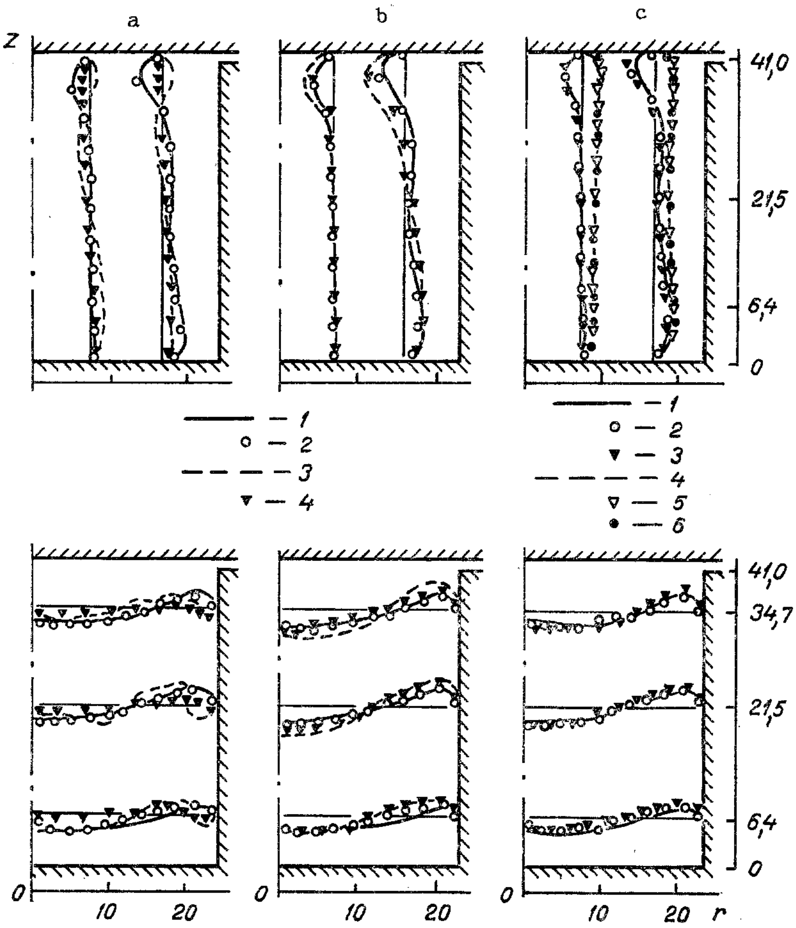

Fig. 2. Comparison of the computed and experimental data [26]: a) modeling of the boundary conditions [1) experiment; 2) calculation with the wall functions; 3) sticking conditions with uniform step; 4) sticking with bunching at the walls]; b) modeling of turbulent viscosity [1) experiment; 2) differential subgrid model; 3) "simplified" subgrid model; 4) $\mu_T = 10^{-3}$]; c) modeling taking into account the roughness of the surfaces and comparison of the rms values $\sqrt{\overline{u^2}}$ with experiment [1) experiment; 2) calculation, smooth surface; 3) calculation, sandy roughness; 4) experiment on rms values $\sqrt{\overline{u^2}}$; 5) differential subgrid model; 6) "simplified" subgrid model]. z, r, mm.

fied" subgrid model (1) or the differential model (2) and (3) were employed or the constant value $u_T = 10^{-3}$ was employed. As a supplement to Fig. 2c (top part) a comparison with respect to the rms values $\sqrt{\overline{u^2}}$, reflecting the contribution of turbulent pulsations (the numbers 4, 5, and 6), are given. Analysis of the distributions presented in Fig. 2b and at the top of Fig. 2c shows that as the piston approaches the top dead point (TDP) the flow is turbulent, and in addition the turbulence can be modeled quite well with a "simplified" subgrid model of turbulence (1), which is an equilibrium variant of the "differential" subgrid model [12]. It should be noted that the intensity of turbulence, according to the calculations, is not uniform over the volume of the cylinder during compression (see the variant with u_T = const), since the generation of turbulence owing to friction at the walls and the effect of the gas jet emanating from the opening above the cylinder in the CC play a significant role during compression.

Under real conditions the internal, nonrubbing surfaces of the CC are not smooth. To answer the question of whether or not it is necessary to take into account the roughness of the surfaces when calculating the gas dynamics of compression, we performed calculations with a sandy roughness on the walls and compared the profiles obtained with the experimental profiles for a CC with smooth walls [26]. As the distributions presented in Fig. 2c show

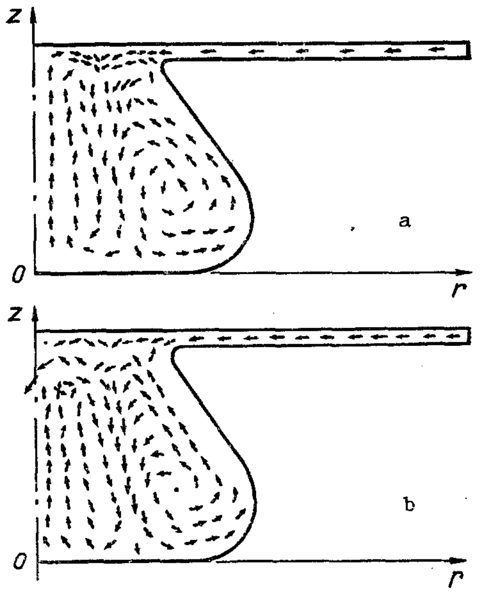

Fig. 3. Comparison of the patterns of flow with identical CCs: a) calculation of the authors; b) calculation of [27] with the help of the RECP-3 program.

the roughness does not significantly affect the average values of the u and v components of the velocity vector.

To make an additional test of the computational algorithm test calculations of the gas dynamics of compression were performed and compared with analogous calculations [27], carried out based on the computational program RECP-3. The experimental data from [5] were employed as the starting velocity distribution, as done in [27]. As follows from Fig. 3, the

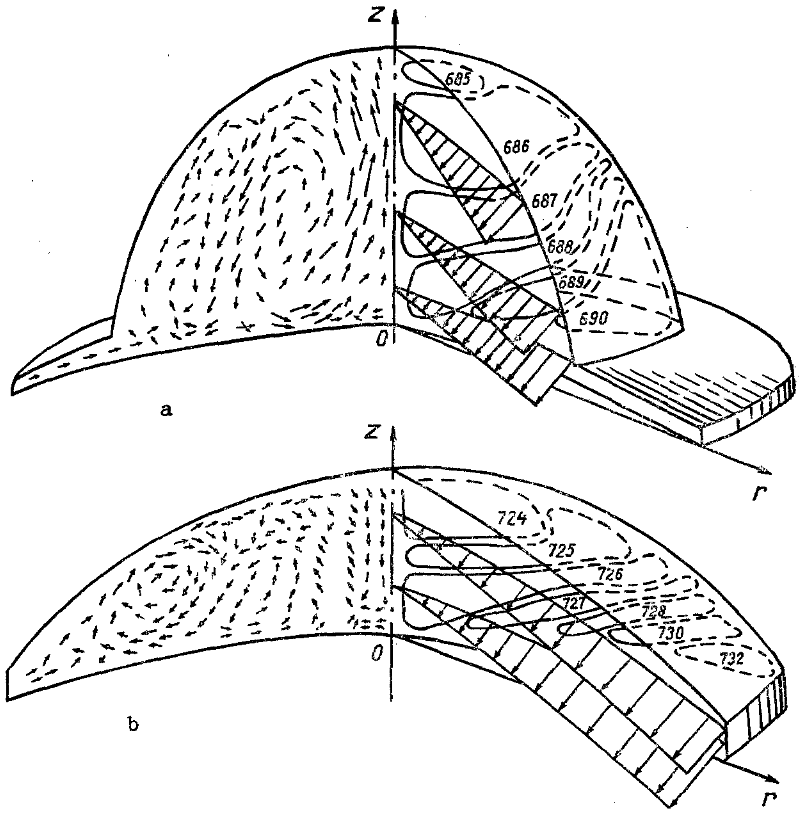

Fig. 4. Configuration of the flow for different forms of the CC with α = 170°; the velocity vectors are shown on the left and the distribution of the isotherms and the azimuthal velocity $\overline{w}$ are shown on the right.

flow patterns are in agreement in the entire region, except near the injector, where a spray of fuel develops (in Fig. 3b the flow pattern taken from [27] is shown at the moment of fuel injection).

Figure 4 shows the velocity and temperature fields and the field of the azimuthal velocity component $\overline{w}$ for two different forms of the surface of the cylinder head. As one can see, the geometry of the CC, shown in Fig. 4a, encourages the appearance of two, oppositely directed, vortices, of which the larger one lies closer to the axis of the cylinder. The variant of the CC shown in Fig. 4b leads to weak formation of vorticity of the charge in the plane of the symmetry axis. One can also see that the magnitudes of the velocity vectors differ significantly. The fuel mixture will be better mixed in the CC shown in Fig. 4a than in the case of the CC shown in Fig. 4b. The figure shows the azimuthal velocity vector w, from whose magnitudes it follows that the configuration of the cylinder heads affects the change in the degree of twisting of the gas charge. Analysis of Fig. 4 demonstrates that a priori calculations of the gas dynamics of compression in designing the form of the CC of a cylinder of a ICE can make effective predictions.

The numerical calculations of the gas dynamics of compression in a cylinder of a ICE show the following: a) under the assumption of a thin boundary layer at the walls, the computational method employed permits predicting with adequate accuracy the configuration of the flow in the CC of the cylinder of a ICE as the piston approaches the TDP; b) the form of the surface of the cylinder head strongly affects the configuration of the flow during the compression process; c) the presence of irregularities on the inner surfaces of the CC does not appreciably affect the pattern of development of the flow; and, d) the degree of turbulent diffusion can be predicted quite well using the "simplified" subgrid model of turbulence. At the same time the intensity of turbulent diffusion is not the same over the entire volume of the cylinder during the compression stroke.

NOTATION

t, time; T_0, starting temperature; μ_T, turbulent viscosity; ρ, density; V_p, velocity of the piston; S, length of the cylinder path; N, number of revolutions of the fly wheel; α, angle of rotation of the crankshaft; d, length of the connecting rod; u, v, longitudinal and transverse components of the velocity.

LITERATURE CITED

1. F. V. Bracco and P. J. O'Rourke, Prog. Energy Combust. Sci., 7, 103-124 (1981).
2. A. D. Gosman, R. J. R. Johns, and A. P. Watkins, Modeling in Reciprocating Engines, New York (1980), pp. 299-326.
3. Yu. M. Davydov, M. G. Kruglov, A. A. Mednov, and V. A. Nefedov, Numerical Investigation of Flows in Internal Combustion Engines by the Method of Large Particles [in Russian], Moscow (1983).
4. P. O. Witze, "Comparisons between measurement and analysis of fluid motion in internal combustion engines," Sandia National Laboratories Energy Report SAND-8242 (1981).
5. W. C. Reynolds, Modeling in Reciprocating Engines, New York (1980), pp. 299-326.
6. A. M. Mellor and S. R. Fergyuson, Turbulent Flows of Reacting Gases [in Russian], Moscow (1983), pp. 85-96.
7. T. D. Butler, L. D. Cloutman, J. K. Kukowics, and J. K. Ramshaw, Prog. Energy Combust. Sci., 7, 293-315 (1981).
8. N. Rumiano and S. Cauffier, Rev. Inst. Fr. Pet., 38, No. 4, 533-543 (1983).
9. M. A. Gorokhovskii and V. P. Khlynin, Inzh.-Fiz. Zh., 51, No. 4, 654-659 (1986).
10. J. W. Deardorff, J. Fluid Mech., 41, 453-467 (1970).
11. J. W. Deardorff, J. Comput. Phys., 7, No. 1, 120-133 (1971).
12. A. A. Amsden, T. D. Butler, P. J. O'Rourke, and J. K. Ramshaw, "KIVA-A comprehensive model for 2-D and 3-D engine simulations," SAE Techn. Paper Ser., 850,554 (1985).
13. M. J. Hall and F. V. Bracco, "Cycle-resolved velocity and turbulence measurements near the cylinder wall of a firing S. I. engine," SAE Techn. Paper Ser., 861,530 (1986).
14. B. E. Launder, A. Morse, W. Rodi, and D. B. Spalding, Proceedings of the Conference on Turbulent Shear Flows, NASA Langley Research Center, NASA SP-321 (1972), pp. 361-426.
15. S. V. Patankar and D. B. Spalding, Heat and Mass Transfer in Boundary Layers, Intertext Books, London (1970).
16. L. K. Cloutman, J. K. Dukowicz, and J. K. Ramshaw, Proceedings of the 7th International Conference on Numerical Methods in Fluid Dynamics, Berlin (1981), pp. 119-124.

17. T. D. Butler, L. K. Cloutman, J. K. Dukowicz, and J. K. Ramshaw, Prog. Energy Combust. Sci., 7, 293-315 (1981).
18. P. O. Witze, Sandia Report N81-8242, Livermore (1981).
19. F. H. Harlow and A. A. Amsden, J. Comp. Phys., 8, 197-213 (1971).
20. W. Rivard, T. Butler, and O. Farmer, Numerical Solution of Problems in Hydromechanics [Russian translation], Moscow (1977).
21. S. Khert, Numerical Methods in Fluid Mechanics [in Russian], Moscow (1973), pp. 156-164.
22. B. D. Dali, Numerical Solution of Problems in Hydromechanics [in Russian], Moscow (1977), No. 14, pp. 143-156.
23. J. F. Thompson, F. C. Thames, and C. W. Mastin, J. Comput. Phys., 15, 299-319 (1974).
24. P. D. Thomas and J. F. Middlekoff, Raket. Tekh. Kosmonavt., 18, No. 7, 55-61 (1980).
25. N. N. Yanenko, N. T. Danaev, and D. V. Liseikin, Numerical Methods in the Mechanics of Continuous Media [in Russian], Novosibirsk (1977), Vol. 8, No. 4, pp. 157-163.
26. C. Arcoumanis, A. F. Bicen, and J. H. Whitelaw, Trans. ASME J. Fluids Eng., 105, 105-112 (1983).
27. C. Bassoli, G. Biaggini, G. Bodritti, and G. M. Cornetti, "Two-dimensional combustion chamber analysis of direct injection diesel," SAE Tech. Paper Ser. (1984).

STRUCTURE OF INHOMOGENEOUS MEDIA WITHIN THE RANDOM FRACTAL MODEL

R. R. Nigmatullin and N. N. Sutugin

UDC 536.7

The porosity of inhomogeneous media is treated within the random fractal model. Analytic expressions are obtained for the size distribution curves of bulk mesopores.

The concepts of a fractal and fractal dimensionality [1] are extremely fruitful in describing the geometry of heterogeneous systems, in the study of percolation effects, properties of various self-similar objects and structures, generated in hydrodynamics, astrophysics, electrochemistry, and other disciplines. More detailed information can be found, for example, in the reviews [2, 3]. The extension of the concept of a regular fractal and the introduction of a set of inhomogeneous objects with distributed values of fractal dimensionality became possible due to the multifractal approach, a topic discussed in the studies [4, 5].

Besides this extended class of regular fractals another is possible, which, as far as we are concerned, is a more natural method of introducing fractals, where the fractal scale, and not its dimensionality, occupies the role of the random fractal. The random fractal model (RFM) is proposed on the basis of the new concept of generalized fractal. The distribution function of various scales is found, and equations are obtained for the porosity of an inhomogeneous medium. The equations for two-phase system concentrations are generalized and interpreted if the distribution of one of the phases is fractal. A more detailed interpretation of experiments, related to measurements of porosity and the proof of their fractal occurrence in sandstones, is given within the RFM [6, 7]. Also analyzed was the size distribution function of bulk mesopores with the purpose of searching regions of fractal structure with its help. Comparison with experiment makes it possible to establish a number of new consequences and indicates internal consistencies of the model.

Description of Heterogeneous Media by Generalized Fractals. By means of some figure we divide the given volume V into original or elementary "volumes" $v_f(\Lambda) = G_f\Lambda^d$ with character-

---

V. I. Ul'yanov (Lenin) Kazan State University. Translated from Inzhenerno Fizicheskii Zhurnal, Vol. 57, No. 2, pp. 291-298, August, 1989. Original article submitted January 1, 1988.

 0022-0841/89/5702-0958$12.50